Gray Molasses on Rubidium-87 atoms

Author: Èlia Solé Cardona

Facultat de Física, Universitat de Barcelona, Diagonal 645, 08028 Barcelona, Spain and
Institut de Ciències Fotòniques, Avinguda Carl Friedrich Gauss 3, 08860 Castelldefels, Spain.

Advisor: Bruno Julia Diaz and Morgan Mitchell/Daniel Benedicto

Abstract: This project presents an experimental study on the implementation of gray molasses cooling in an ultracold ^{87}Rb experiment. Gray molasses, a sub-Doppler cooling technique, effectively increases the phase-space density of cold trapped atoms by utilizing dark and bright states. We present a theoretical view of the technique, as well as a description of the experimental setup and the modifications required for implementing the technique on ^{87}Rb. The results reveal temperatures as low as $8,64\mu$K and a phase-space density of $1,97 \cdot 10^{-8}$, in a sample of $1,3 \cdot 10^6$ atoms.

I. INTRODUCTION

Laser cooling is a general term encompassing many techniques that use atom-light interactions to achieve cold temperatures close to absolute zero in atomic and molecular gases. It was first proposed in the late 1970s and its pioneers won the Nobel Prize in Physics in 1997 [1]. Laser cooling is an indispensable tool in ultracold atomic experiments, a platform that has proven its qualities for investigating phenomena in the fields of quantum optics and quantum many-body physics.
By absorbing and subsequently re-emitting photons, atoms reduce their kinetic energy, leading to a decrease in temperature. Doppler cooling techniques employ the Doppler effect for cooling atoms. The recoil energy, i.e. the photon momentum transferred to the atoms during the scattering process, sets a lower bound on the achievable temperature. To surpass this limit, sub-Doppler cooling techniques have been developed [2], which employ light-polarization gradients and optical pumping to cool atomic gases below the Doppler cooling limit [3]. The work focuses on a sub-Doppler cooling technique called gray molasses. This technique relies on the existence of states that do not interact with the laser light, i.e. dark states, and it has been demonstrated in various atomic species, including Cs [4], K [5], and Rb [6].

In this work, we present the results of our experimental implementation of the gray molasses cooling technique in an ultracold ensemble of ^{87}Rb. The motivation is to enhance the loading of atoms into an optical dipole trap. Gray molasses implementations have shown increased loading efficiency by reducing the temperature and increasing the density of the atomic cloud [7]. We begin by providing the theoretical foundations of the cooling mechanism in Section II. In Section III, we describe the experimental setup. We explain the process of obtaining atomic cloud parameters using fluorescence imaging and provide a step-by-step description of the experimental sequence. Then, in Section IV, we present the experimental results obtained from the implementation of the gray molasses technique. Finally, In Section V we discuss the results.

II. GRAY MOLASSES

Doppler cooling techniques rely on the interaction between atoms and resonant laser radiation. A counter-propagating laser can slow down atoms in an atomic beam by having the atoms absorb and spontaneously emit light. Each absorbed photon imparts a momentum kick to the atom in the opposite direction of its motion, followed by the spontaneous emission of a photon in a random direction. This scattering process, occurring over many absorption-emission cycles, leads to an average force that decelerates the atoms. The process requires closed atomic transitions, where the atoms are at all times interacting with the laser field. In contrast, the gray molasses technique benefits from the existence of dark states. Dark states exist, regardless of the polarization, in transitions $F \rightarrow F'$ between ground (F) and excited ($F'(\leq F)$) atomic states.
To illustrate the technique we consider atoms with an atomic Λ-type energy structure, i.e. an energy level configuration with two ground states and an excited state. The simplified one-dimensional arrangement consists of two counter-propagating bichromatic laser beams with perpendicular linear polarizations. They form an intensity and polarization gradient in space. This results in periodic light shifts of the bright states, allowing the cooling mechanism depicted in Figure 1. In order to effectively cool down the atoms, the energy of the bright states must be higher than that of the dark states. This energy difference is achieved by using lasers that are blue-detuned from the transition. Blue(red)-detuned light has a higher(lower) frequency compared to resonant light. As a result, a moving atom climbs the potential hill created by the bright states, losing kinetic energy until they are optically pumped back into the dark state. The optical pumping process involves the absorption of the laser light, transitioning to the excited state and spontaneously emitting a photon. The interesting feature of this arrangement is that it allows a population transfer from the dark state to the bright state, via a non-adiabatic passage primarily at the potential minima of the bright states, as seen theoretically in [8]. This introduces a gray character to the dark state since the atoms can still tran-

sition to a bright state. The probability of this transfer increases with atomic velocity, leading to the accumulation of slow atoms in the dark state, where photon scattering is suppressed. On the other hand, fast atoms are transferred to a bright state and undergo the cooling cycle.
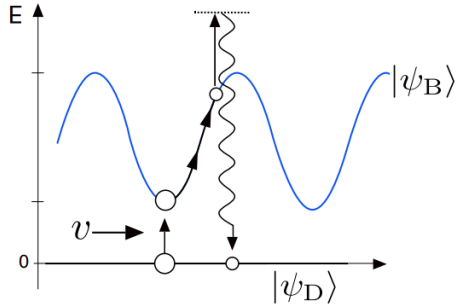
FIG. 1: Gray molasses cooling scheme [8]. An atom in the dark state $|\Psi_D\rangle$ undergoes velocity-induced coupling and is transferred to the bottom of the bright state $|\Psi_B\rangle$ potential. While climbing the potential, the atom loses kinetic until they are transferred back to the dark state, with a cycle of absorption and spontaneous emission of light.

Until now, our discussion has revolved around a basic three-level scheme. However, in order to gain a deeper understanding of the gray molasses cooling mechanism, we employ a model that follows the approach outlined in [9]. The atom-light interaction in the system is described by a Hamiltonian of the form $H = H_0 + H_C$, where H_0 is the Hamiltonian of the free atom, and H_C is the atom-light coupling Hamiltonian. For ^{87}Rb, gray molasses can be achieved in the D_2 line and the laser light addresses transitions between $|F = 1, 2\rangle$ to $|F' = 2\rangle$. The light field consists of two different frequencies, shown in Figure 2. The expression for H_0 is given by [9]:

$$H_0/\hbar = \sum_m |F = 2, m\rangle(\Delta_{22} - \Delta_R)\langle F = 2, m|$$

$$+ \sum_{m'} |F' = 2, m'\rangle(\Delta_{22})\langle F' = 2, m'| \tag{1}$$

H_c is given by:

$$H_c/\hbar = \sum_{m,\sigma,m'} [C_{F=1,m,\sigma,F'=2,m'}\, \Omega_{F=1,\sigma}(z)\, |1, m\rangle\langle 2, m'|$$

$$+ C_{2,m,\sigma,2,m'}\Omega_{F=2,\sigma}(z)|2, m\rangle\langle 2, m'|\,] + \text{h.c.} \tag{2}$$

Where $C_{F,m,\sigma,F',m'}$ are the relevant Clebsch-Gordan coefficients for the transitions and $\Omega_{F,\sigma}(z)$ is the position-dependent Rabi frequencies. The Hamiltonian yields a similar physical depiction to that of the simplified Λ-configuration.

III.   METHODOLOGY

As reviewed in the last section, gray molasses cooling can be achieved on the D_2 line of ^{87}Rb [6], which corresponds to transitions between the ground state $5S_{1/2}$ and the excited state $5P_{3/2}$. The cooling is efficient due to the large hyperfine separation between excited $|F' = 2\rangle$ and $|F' = 3\rangle$ sublevels. Figure 2 illustrates the two laser frequency configurations used for two different stages of the experimental sequence: the magneto-optical trap (MOT) and the gray molasses. The MOT is used as a preparation stage for the gray molasses. It combines optical and magnetic fields to cool and trap the atoms in space [10]. It's formed by three orthogonal pairs of counter-propagating lasers with circular polarization. A pair of coils in anti-Helmholtz configuration produce a quadrupole magnetic field with a gradient at the center of ~ 10 G/cm. The lasers intersect at the center of the quadrupole magnetic field. Although the lasers are labeled cooler and repumper in both processes, they do not play the same role in the two techniques. For the MOT, the role of the repumper is to close the transition, optically pumping the atoms to $|F' = 2\rangle$ so they re-enter the cooling cycle. In the gray molasses, the repumper light enhances the cooling providing a new dark and bright state manifold in which gray molasses cooling can occur.
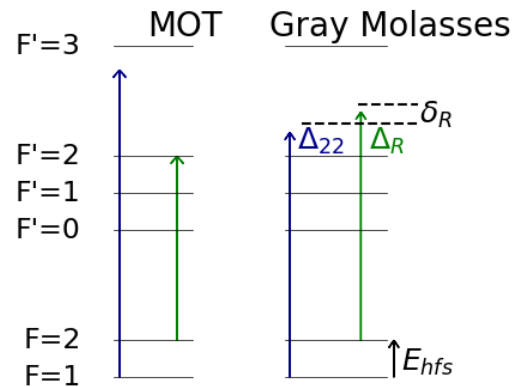
FIG. 2: Atomic level scheme of ^{87}Rb D_2 line illustrating the lasers employed during the Gray Molasses and MOT phases of the experimental sequence: cooler (blue) and repumper (green). For the MOT: the cooler is red detuned from $|F = 2\rangle \rightarrow |F' = 3\rangle$ and repumper is resonant with $|F = 1\rangle \rightarrow |F' = 2\rangle$. For gray molasses: the cooler(repumper) laser is blue detuned with respect to $|F = 2(1)\rangle \rightarrow |F' = 2\rangle$, with detuning Δ_{22} (Δ_R). The relative detuning between the repumper and the cooler light is δ_R. $E_{hfs} = 6.834$ GHz is the energy splitting between the two hyperfine states of the atomic ground state.

The experimental setup is described in [11]. Here, we will discuss the laser system and how it has been modified for the implementation of the gray molasses technique. The laser system used in this study is described as follows: a master laser operating at a

wavelength of 1560 nm is frequency-doubled and locked to the $|F = 2\rangle \rightarrow |F' = 3\rangle$ atomic transition using modulation transfer spectroscopy [12]. Two diode lasers are employed to generate the repumper and cooler light, with their frequencies locked with respect to the master laser frequency using an offset-lock technique [13]. During the gray molasses stage, it has been demonstrated that the cooling mechanism is enhanced when both repumper and cooler lights are coherent [6]. In our experimental configuration, we achieve this by employing an Electro-Optical Modulator (EOM) (WPM-K0780-P85P85AL0-21062181, AdvR) to modulate the phase of the cooler light. Hence, the repumper light for the molasses phase is obtained as a sideband of the cooler light. The output frequency is adjusted by VCO(2) while keeping the VCO(1) signal fixed at 300 MHz. The relationship between the tuning voltage and the output frequency of VCO(2) is depicted in Figure 4. The frequency that drives the EOM (Δ_{RC}) determines the frequency difference between the cooler and the created repumper, and is defined as $\Delta_{RC} = \Delta_R - \Delta_{22} + E_{hfs}/\hbar$ where $E_{hfs} = 6.834$ GHz. On the other hand, the power of the radio-frequency determines the intensity ratio between the cooler and the repumper I_R/I_C and is adjusted using a voltage-variable attenuator (VVA). The calibration of the intensity ratio is presented in Figure 4.

We use fluorescence imaging to extract parameters of the atomic cloud. The technique consists of collecting the fluorescence from the atomic cloud while it is driven by near-resonant light. We use a simple imaging system and a CCD camera to take pictures of the cloud. The number of atoms can be obtained from the brightness of the fluorescence image given by $N_{\text{counts}}/(R_{sc}d\Omega t_{\text{exp}}\eta_{\text{counts}})$ [14], where N_{counts} is the number of counts made by the CCD camera, t_{exp} the exposure time, η_{counts} (counts/photon) the CCD efficiency, R_{sc} the scattering rate of the atoms, and $d\Omega$ the solid angle.

We fit the image to a 2D Gaussian distribution and get the size of the atom cloud σ_i (with $i = x, y$ corresponding to the two accessible spatial directions). This allows the estimation of the temperature of the cloud using the time-of-flight technique (TOF). The TOF method consists of turning off all lasers, allowing the atoms to freely expand for a few milliseconds. Afterward, the laser beams are switched on and the pictures are taken. The evolution of the cloud size with respect to the TOF duration t_{tof} is described by the equation [6, 14]:

$$\sigma_i^2(t_{\text{tof}}) = (\sigma_i^0)^2 + (k_B T_i/m)t_{\text{tof}}^2 \tag{3}$$

Where σ_i^0 is the initial size of the cloud before expansion, m is the atom mass, and k_B is the Boltzmann constant. Figure 5 shows a typical set of experimental data to obtain the temperature of the atomic cloud.
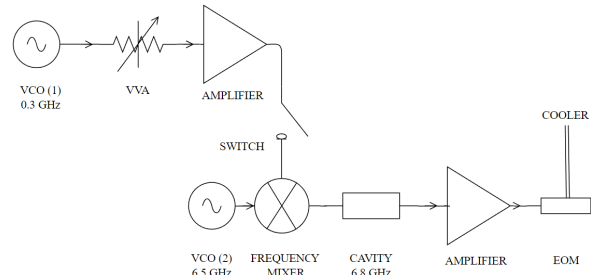
FIG. 3: Schematic representation of the radio-frequency creation setup used to drive the EOM. A voltage-controlled oscillator VCO(1) creates a 0.3 GHz signal, attenuated through a voltage variable attenuator (VVA) and later amplified. This signal goes through a Switch, that allows it to pass when voltage is applied. The VCO(2) creates a tunable signal around 6.5 GHz. A frequency mixer produces an output that contains the sum and difference frequencies of the two VCO signals. A cavity filters out the undesired frequency and the 6.8 GHz signal is amplified and fed to the EOM.
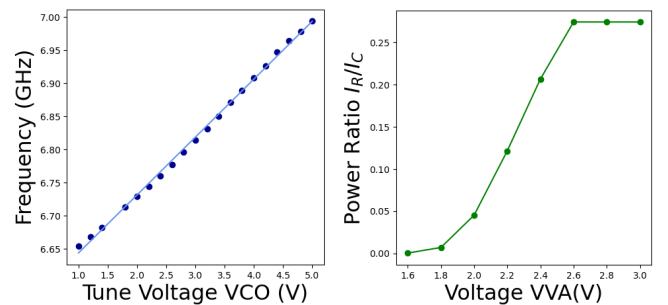
FIG. 4: Left: Output frequency as a function of the tuning voltage of the VCO(2). A linear fit to the data gives a tuning sensitivity of 87.4(5) MHz/Volts. Right: Ratio between the intensity of the repumper and the cooler laser as a function of the voltage applied to the VVA. The repumper light is obtained as a sideband of the cooler using an EOM. The ratio is calculated as $I_R/I_C = [J_1(\gamma)/J_0(\gamma)]^2$, where $J_n(x)$ are the Bessel function. The modulation depth (γ) depends on the applied driving power (V_a) in volts: $\gamma = \pi V_a/(2V_\pi)$, where V_π is the half-wave voltage and is given in the specifications of the EOM.
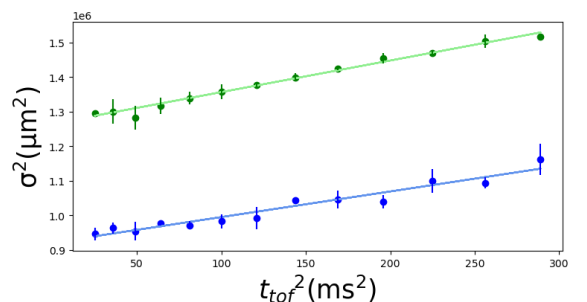
FIG. 5: Size of the atom cloud squared dependence on the squared time of flight duration, with $\sigma_{x(y)}$ in blue(green). Error bars are the standard deviation from 3 repetitions of the experiment. The linear fit using the time-of-flight method obtains $T_x = 7.74(0)$ μK and $T_y = 9.54(8)$ μK, making the average $T = 8.64(4)$ μK.

A.   Experimental Sequence

The experimental sequence is illustrated in Figure 6, providing a visual representation of the time evolution of some key parameters. We start loading a magneto-optical trap for t_{MOT} seconds. For the MOT stage, the two counter-propagating beams in the horizontal plane have powers of approximately 7 mW and in the vertical direction around 9 mW. For the gray molasses step, the magnetic field gradient is turned off and the frequency of the cooler is ramped in 2 ms. We ramp to a value of $\Delta_{22} = 11\Gamma$ detuning from the $F = 1 \rightarrow F' = 2$ transition, where $\Gamma = 6.6$ MHz is the natural linewidth of the D_2 line for ^{87}Rb. Simultaneously, the repumper light used for the MOT loading is switched off, and the coherent repumper is generated through the EOM. Following this, the gray molasses is initiated by ramping the optical power for 6 ms. It starts from a large optical intensity, allowing for the capture of a substantial number of atoms from the MOT. Then, all laser beams are extinguished, enabling the free expansion of the trapped atoms for a time-of-flight t_{tof}. Within this interval, the frequency of the cooler laser is ramped to the MOT stage frequency in 4 ms. For imaging, the frequency of the cooler is tuned to resonance with the $F = 2 \rightarrow F' = 3$ transition.
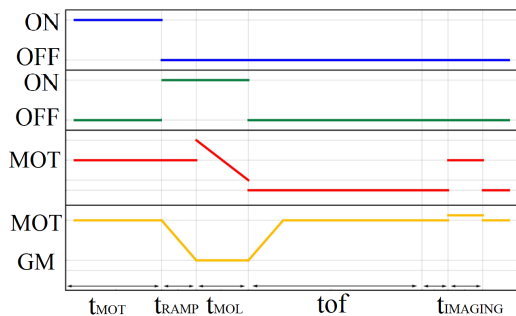
FIG. 6: Experimental sequence with the time dependencies of various parameters: the quadrupole magnetic field (blue), the coherent repumper switch (green), the total optical power of the laser beams (red), and the cooler frequency (yellow). We load the MOT for t_{MOT}. Then, we switch off the quadrupole magnetic field and ramp in t_{ramp} the frequency of the cooler to Δ_{22} detuned from the $F = 1 \rightarrow F' = 2$ transition. We switch on the radio-frequency creation setup and the repumper laser is created by the EOM. The duration of the gray molasses is t_{mol}. Then, we switch off the laser lights and let the atoms freely expand for t_{tof}. While this is happening, we ramp the frequency of the cooler back to the value needed for the MOT loading. Before acquiring the fluorescence image of the atoms, the frequency of the cooler is set to the resonance of the $F = 2 \rightarrow F' = 3$ transition .

IV.   RESULTS

In this section, we present the results obtained from our experimental study. We began examining the impact

of varying the Raman detuning, i.e. the relative detuning between the repumper and the cooler light defined as $\delta_{\text{R}} = \Delta_{\text{R}} - \Delta_{22}$. This is achieved by changing the driving frequency of the EOM, as seen in Figure 4. The data obtained for a fixed value of $\Delta_{22} = 11\Gamma$ and $I_{\text{R}}/I_{\text{C}} = 0.02$ is shown in Figure 7. The duration of the molasses stage was set to $t_{MOL} = 6ms$. We find the minimum temperature achieved when $\delta_{\text{R}} = -0.04\Gamma$, slightly below the Raman condition ($\delta_{\text{R}} = 0$). This is consistent with previous observations [6].
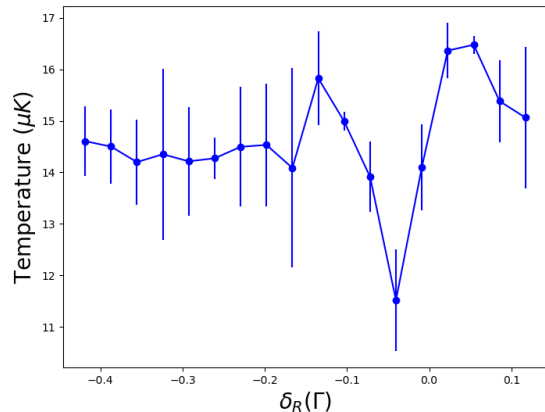
FIG. 7: Temperature as a function of Raman detuning. The temperature is measured using the TOF method with only one data point with $t_{\text{tof}} = 12$ms. The error bars are the standard deviation from 4 repetitions of the experiment. The minimum temperature is achieved at $\delta_R = -0.04\Gamma$.

We conducted further analyses by varying the ratio between the intensities of the repumper and cooler lasers, denoted as $I_{\text{R}}/I_{\text{C}}$, with characterization shown in Figure 4. The number of atoms and temperature were measured using the fluorescence imaging described in the previous section. The results of our analysis are shown in Figure 8. For this data collection the Raman detuning is set to the optimal value $\delta_{\text{R}} = -0.04\Gamma$ with the other parameters kept the same as for the data in Figure 7. The number of atoms stays constant with the intensity ratio, at a value $N \approx 1.5 \cdot 10^6$ atoms. The intensity ratio has an effect on the temperature, with the minimum reached for an intensity ratio $I_{\text{R}}/I_{\text{C}} \approx 20\%$. Our findings align with earlier studies conducted on ^{87}Rb [6].

As a final study, we compare the results of the gray molasses technique in our experimental setup with the bright molasses technique, which was the cooling technique already implemented in the experiment. As a figure of merit, we use the phase space density (PSD). The PSD of an atomic cloud characterized by the number of atoms N at an average temperature T and a size σ_i can be expressed as [10]: $\text{PSD} = n_i \left[(h^2)/(2\pi m K_B T_i) \right]^{3/2}$. Where n_i is the number density of the molasses $n_i = N/(2\pi(\sigma_x \sigma_y)^{3/2})$.
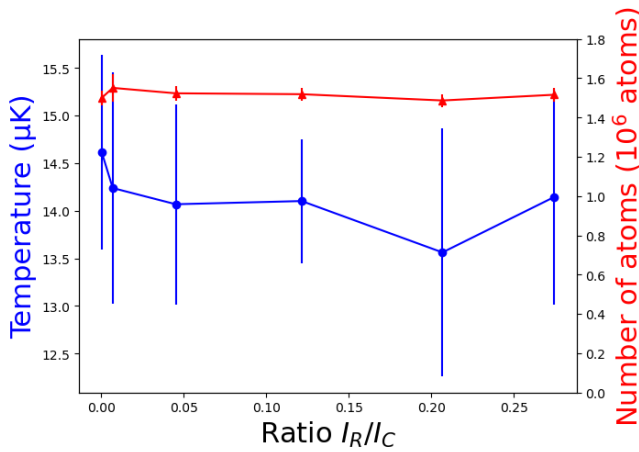
FIG. 8: Temperature (blue) and number of atoms (red) as a function of the intensity ratio between the repumper and cooler laser. The temperature is measured using the TOF method with only one data point with $t_{\text{tof}} = 12$ms. Error bars are the standard deviation from 5 repetitions of the experiment. The optimal parameter is $I_{\text{R}}/I_{\text{C}} = 20\%$, corresponding to a radio-frequency attenuation of 2.4 V.

	T (μK)	PSD
Bright Molasses	6.75(4)	2.50(6) $\times 10^{-8}$
GM $\delta_r = -0.14\Gamma$	10.40(7)	1.35(7) $\times 10^{-8}$
GM $\delta_r = -0.04\Gamma$	8.64(4)	1.97(3) $\times 10^{-8}$
GM $\delta_r = +0.12\Gamma$	9.46(0)	1.48(1) $\times 10^{-8}$

TABLE I: Temperature measured using the time-of-flight method and phase space density of the system under different cooling techniques: bright molasses and grey molasses with varying Raman detuning.

V. CONCLUSIONS

In conclusion, our study of the gray molasses sub-Doppler cooling technique in the D_2 line of ^{87}Rb has provided valuable insights into its efficiency for achieving cold temperatures and high phase-space density (PSD). Experimental findings indicate that, compared to the results obtained with bright molasses, the gray molasses did not yield better outcomes under the specific experimental conditions and parameters investigated. This suggests that additional optimization of the experimental parameters is necessary to improve its performance. Our results demonstrated that the Raman detuning played a crucial role in determining the cooling effectiveness of the gray molasses technique. By adjusting the detuning of the repumper light, we observed variations in the temperature and PSD of the atomic ensemble. Notably, the minimum temperature was obtained when the Raman detuning was set slightly below the Raman condition in accordance with previous experimental investigations [6].

[1] Chu, S. (1998). Nobel Lecture: The Manipulation of Neutral Particles. *Rev. Mod. Phys.* **70**(3), 685-706.

[2] Lett, P. D., et al. (1988). Observation of Atoms Laser Cooled Below the Doppler Limit. *Phys. Rev. Lett.* **61**(2), 169-172.

[3] Dalibard, J., and Cohen-Tannoudji, C. (1989). Laser cooling below the Doppler limit by polarization gradients: Simple theoretical models. *J. Opt. Soc. Am. B* **6**, 2023-2045.

[4] Boiron, D., et al. (1995). Three-dimensional cooling of cesium atoms in four-beam gray optical molasses. *Phys. Rev. A* **52**(5), R3425-R3428.

[5] Salomon, G., et al. (2014). Gray-molasses cooling of ^{39}K to a high phase-space density. *EPL (Europhys. Lett.)* **104**(6), 63002.

[6] Rosi, S., et al. (2018). Λ-enhanced grey molasses on the D2 transition of Rubidium-87 atoms. *Sci. Rep.* **8**, 1301.

[7] Naik, D. S., et al. (2020). Loading and cooling in an optical trap via hyperfine dark states. *Phys. Rev. Res.* **2**(1), 013178.

[8] Weidemüller, M., et al. (1994). A Novel Scheme for Efficient Cooling below the Photon Recoil Limit. *EPL (Europhys. Lett.)* **27**(2), 109-114.

[9] Bruce, G. D., et al. (2017). Sub-Doppler laser cooling of ^{40}K with Raman gray molasses on the D2 line. *J. Phys. B: At. Mol. Opt. Phys.* **50**(9), 095002.

[10] Foot, C. J. (2005). Atomic Physics. *Oxford Master Series in Physics*.

[11] Palacios, S., et al. (2018). Multi-second magnetic coherence in a single domain spinor Bose-Einstein condensate. *New J. Phys.* **20**, 053008.

[12] de Escobar, Y., et al. (2015). Absolute Frequency References at 1529 nm and 1560 nm Using Modulation Transfer Spectroscopy. *arXiv*.

[13] Appel, J., et al. (2009). A versatile digital GHz phase lock for external cavity diode lasers. *Meas. Sci. Technol.* **20**(5), 055302.

[14] Perea-Ortiz, M. (2015). Progress towards a quantum simulator with cold atoms. *PhD thesis, University of Birmingham*.